

The effects of peak ground velocity of near-field ground motions on the seismic responses of base-isolated structures mounted on friction bearings

H.Tajammolian^{1a}, F.Khoshnoudian^{*2}, S.Talaei³ and V.Loghman³

¹Structural Engineering, Structural Engineering, Faculty of Civil Engineering, Amirkabir University of Technology, Tehran, Iran

²Faculty of Civil Engineering, Amirkabir University of Technology, Tehran, Iran

³Earthquake Engineering, Faculty of Civil Engineering, Amirkabir University of Technology, Tehran, Iran

(Received April 20, 2014, Revised May 6, 2014, Accepted May 7, 2014)

Abstract. This research has been conducted in order to investigate the effects of peak ground velocity (PGV) of near-field earthquakes on base-isolated structures mounted on Single Friction Pendulum (SFP), Double Concave Friction Pendulum (DCFP) and Triple Concave Friction Pendulum (TCFP) bearings. Seismic responses of base-isolated structures subjected to simplified near field pulses including the forward directivity and the fling step pulses are considered in this study.

Behaviour of a two dimensional single story structure mounting on SFP, DCFP and TCFP isolators investigated employing a variety range of isolators and the velocity (PGV) of the forward directivity and the fling step pulses as the main variables of the near field earthquakes. The maximum isolator displacement and base shear are selected as main seismic responses. Peak seismic responses of different isolator types are compared to emphasize the efficiency of each one under near field earthquakes. It is demonstrated that rising the PGVs increases the isolator displacement and base shear of structure. The effects of the forward directivity are greater than the fling step pulses. Furthermore, TCFP isolator is more effective to control the near field effects than the other friction pendulum isolators are. This efficiency is more significant in pulses with longer period and greater PGVs.

Keywords: near field ground motions; simplified pulse models; seismic isolation; friction isolators

1. Introduction

Near field effects on different structures are one of the interesting subjects in earthquake engineering. Previous researches show that the ground motions are significantly affected by fault

*Corresponding author, Associate Professor, Email: Khoshnud@aut.ac.ir

^aPh.D Candidate

^bMsc Graduated

^cMsc Graduated

mechanism. Direction of rupture propagation relative to the site e.g., forward directivity and the possible static deformation of the ground surface associated with fling-step effects are well-known phenomena in near field earthquakes (Kalkan and Kunnath 2006). The effects of the fling step and the forward directivity pulses on structures as well as replacing them with mathematically idealized simple pulses have always been an interesting issue for different researchers in near-field earthquakes studies.

The impact of near-field earthquakes on different types of buildings investigated by Mahin *et al.* (1976), Bertero *et al.* (1978), Anderson and Bertero (1978) and Mahin and Bertero (1981). Krawinkler and Alavi (1998) applied pulse models with triangular shape to model near-field earthquakes. Agrawal and He (2002) used sinusoidal pulses for a similar aim. Sasani and Bertero (2000) substituted the fling step and the forward directivity ground motions with sinusoidal pulses. Backer (2007) extracted forward directivity pulses from actual near-field earthquakes for ninety one near-field records employing wavelet analysis.

Kalkan and Kunnath (2006) investigated the seismic response of structures subjected to the fling step and the forward directivity ground motions with idealized sinusoidal pulses. In this study, authors have revealed that near-fault motions caused by forward directivity effects lead to more damages comparing to fling step pulses. In addition, it was demonstrated that although idealized simple pulses do not contain all the characteristics of real earthquakes, they can provide a reliable relationship between pulse intensity, system characteristics and demands. Khoshnoudian and Ahmadi (2013) applied sinusoidal pulses to study the effects of near-field earthquakes considering soil-structure interaction systems.

Single Friction pendulum isolators (SFP) was introduced and developed by Zayas *et al.* (1987, 1989). Constantinou *et al.* (1993) studied this technology employing in bridges (Fig. 1a). The SFP bearing was improved by adding another sliding surface to the isolation system named as Double Concave Friction Pendulum (DCFP) isolator (Fig. 1b) which can provide greater displacement capacity in comparison to the SFP isolator subjected to strong earthquakes. These two friction concave plates which are placed at the top and the bottom of DCFP isolator may have similar or different radius and also frictional properties. The different aspects of this type of isolator were investigated by different researchers. Hyakuda *et al.* (2001) developed force-displacement equations of this isolator. Their studies focused on the bearings with two concave plates that have equal friction coefficients. Tsai *et al.* (2005) examined a 4-story superstructure mounted on DCFP isolators. They suggested utilizing an articulated slider instead of simple slider between two concave plates. The shaking table tests reveal that the DCFP isolator can reduce super-structure acceleration more than 70 percent in comparison with a fixed-base structure. Fenz and Constantinou (2006) proposed a new method for modeling and analysing of the DCFP isolators. They used two SFP bearings connected in series to produce force-displacement behaviour curve for DCFP isolators. Their proposed model can be utilized for isolators with different radius and friction coefficients. Kim and Yun (2007) compared behaviour of DCFP isolators with bi-linear behaviour to isolators with tri-linear behaviour employed in bridges. They concluded that tri-linear isolators can reduce the bridge base shear 15-40 percent comparing to bi-linear ones. Khoshnoudian and Rabie (2010) investigated the effect of vertical component of earthquake on the seismic behaviour of DCFP isolator. They revealed that neglecting the vertical component causes maximum 5 and 22 percent errors in estimating the displacement and base shear of base-isolated structures, respectively. Khoshnoudian and Hemmati (2011) performed a vast parametric study on DCFP isolators. They investigated the effects of superstructure period, isolator's effective periods

and isolator friction coefficients on the responses of isolated structures. This study consequence demonstrated that tri-linear curve isolators cause larger displacement than bi-linear ones.

Recently developed friction isolator; Triple Concave Friction Pendulum (TCFP) can behave in a multi-regimes of movements in different earthquake hazard levels. TCFP isolator can show a compatible behaviour with earthquake intensity. This type of isolators consists of external top and bottom plates and internal ones; employing an articulated slider which separates the bottom plates from the top ones (Fig. 1c). Different issues of TCFP isolator behaviour were studied by Fenz and Constantinou (2008a,b,c,d). They derived force-displacement equations of TCFP isolators; in addition, several experimental tests were performed in their studies. In addition, three SFP elements connected in series were proposed for modeling and analysing of this type of bearing. They have verified the results of this series model with experimental tests responses. Fadi and Constantinou (2009) studied the usage of Equivalent Lateral Force (ELF) procedure of ASCE standard for determination of maximum bearing displacement and superstructure base shear of TCFP systems. They confirmed that ELF method can lead to responses greater than the results of nonlinear analysis. Morgan and Mahin (2010, 2011) presented analytical and experimental investigation on different stages of TCFP responses. They used these results as a framework to describe damage state limitations over multiple levels of seismic hazard. Becker and Mahin (2012) suggested a new model for analysis of this type of bearing. The new model is capable of analyzing the TCFP for two perpendicular earthquake components. Loghman *et al.* (2013) examined the effect of earthquake vertical acceleration on different responses of structures mounted on TCFP isolators. They have accomplished that ignoring the vertical component leads to significant errors in base shear of low-rise superstructures; however, base shear of medium height structures is not be affected. Also, the effect of vertical component of ground motion on the displacement of TCFP isolator is not remarkable. Dao *et al.* (2013) proposed a new model that can analyze the TCFP isolator in three-dimensional earthquake components. They validated their analytical model using the results of 5-story full-scale structure on a shaking table test subjected to different earthquakes.

Wang *et al.* (2013) proposed algorithms for damage assessment of isolators in base-isolated

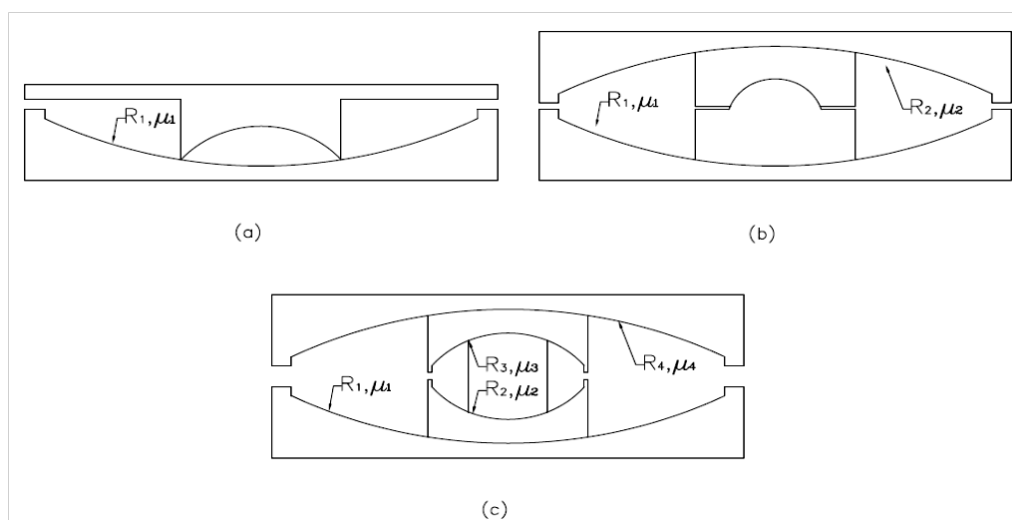


Fig. 1 (a) SFP; (b) DCFP; (c) TCFP bearings (Morgan and Mahin 2010)

building considering torsion-coupling effects. They proposed damage indices, which are able to detect the damage and prepare estimation about the damaged isolator location. Takewaki *et al.* (2013) have compared two types of common dampers used in base-isolated buildings. They studied base-isolated buildings with viscous-type damper and elastic-plastic hysteresis-type. Their investigation reveals that in long-duration earthquakes the responses of isolated building elastic-plastic hysteresis damper becomes larger than the building with other damper type.

This research focuses on the effect of the near-fault PGV pulses on the seismic responses of structures mounted on SFP, DCFP and TCFP isolators which has not been addressed in the previous investigations. An extensive parametric study has been performed using essential parameters such as effective damping and period of SFP, DCFP and TCFP bearings as well as superstructure first mode period. The results of each analysis are compared employing two types of well-known near field ground motions i.e. the forward directivity and the fling step, extensively. Finally, an elaborate comparison between performances of three types of isolators is carried out.

2. Mathematical pulse models for near-field earthquakes

Near field ground motions can exhibit the dynamic consequences of “fling-step” or “forward-directivity” depending on tectonic displacement of the fault, the rupture mechanism and slip

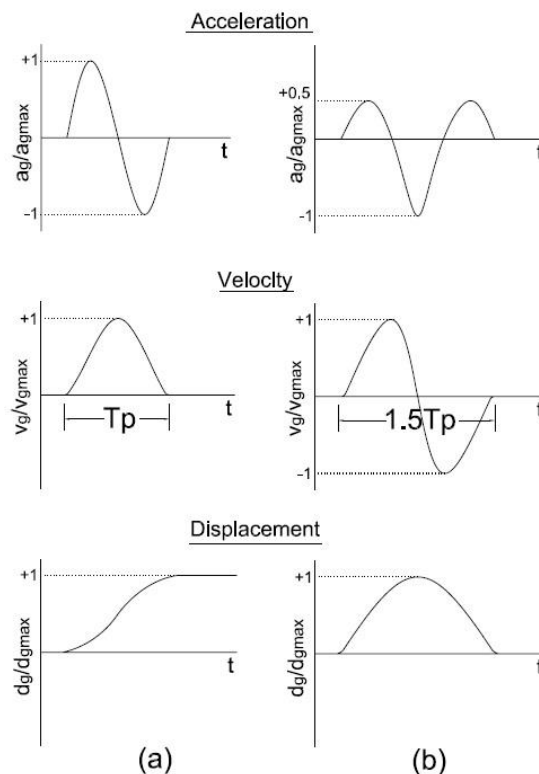


Fig. 2 Idealized sinusoidal pulses (a) fling step pulse (b) forward directivity pulse (Sasani and Bertero 2000)

direction relative to the site (Somerville 1998). The fling-step motion normally generates permanent static displacement which occurs parallel to strike of the fault with strike-slip earthquakes and in the dip direction for dip-slip events; while the forward directivity effect is characterized by a large pulse occurring at the beginning of the motion to be oriented in a direction perpendicular to the fault plane (Somerville 1998). Despite their different dynamic specifications, the near-fault pulse-type ground motions can be represented and quantified by one or more simplified pulses.

Many researchers used these mathematical pulses in their studies. Sasani and Bertero (2000) and Alavai and Krawinkler (2004) investigated simple sinusoidal pulses instead of using actual earthquake records. They showed that employing these pulses can precisely simulate near-fault earthquake effects. Kalkan and Kunnath (2006) applied these pulses to obtain higher modes effects on structures. Khoshnoudian and Ahmadi (2013) utilized these pulses to study the near fault effects on MDOF structures considering soil-structure interaction.

Applied sinusoidal pulses and their velocity and displacement time histories for both the forward directivity and the fling step pulses are depicted in Fig. 2.

According to Fig. 2a, there is a static residual displacement at the end of the fling step displacements time history which is the effect of ground displacement at the fault location. It is verified that the forward directivity pulses period is generally 1.5 to 2.5 times the fling step pulses period (Kalkan and Kunnath 2006). So, in this investigation the pulse period of the forward directivity is considered 1.5 times the fling step which is the minimum value in this range and is compatible with the previous studies (Kalkan and Kunnath 2006, Khoshnoudian and Ahmadi 2013).

It is obvious that the pulse period and pulse amplitude are the most important parameters of the pulse characteristics; therefore, this investigation is performed in order to study the effect of pulse amplitude on the seismic responses of base-isolated structures considering an extensive range of PGVs varies from 20 to 220 cm/s. In this case, to focus the effects of PGVs, only short range of period pulses are chosen which change from 0.5s to 2.5s. This range coincides with the previous studies e.g. Khoshnoudian and Ahmadi (2013).

3. Seismic behavior of SFP, TCFP and DCFP Isolators

Hysteresis loops of friction isolation systems are illustrated in Fig. 3. The seismic behavior of the SFP isolators with a bi-linear hysteresis loops is shown in Fig. 3a.

A DCFP isolation system can have two different types of hysteresis loop. If top and bottom surfaces of a DCFP isolator have equal coefficient of friction it behaves like a SFP isolator and experiences a bi-linear hysteresis loop (Fig. 3a); otherwise choosing different coefficient of friction for top and bottom surfaces of a DCFP isolator changes its behavior to a tri-linear hysteresis curve (Fig. 3b).

Hysteresis behavior of TCFP isolators are much more complicated than the others and can have 5 different regimes of movements which differentiates with two stiffening parts in IV and V regimes of its movements when the isolators experiences a fully adaptive behavior. In this case, the friction coefficient of inner and outer top and bottom surfaces must be $\mu_2 = \mu_3 < \mu_1 < \mu_4$ (Fig. 3c). These stiffness parts are the main difference between the TCFP and the other isolators.

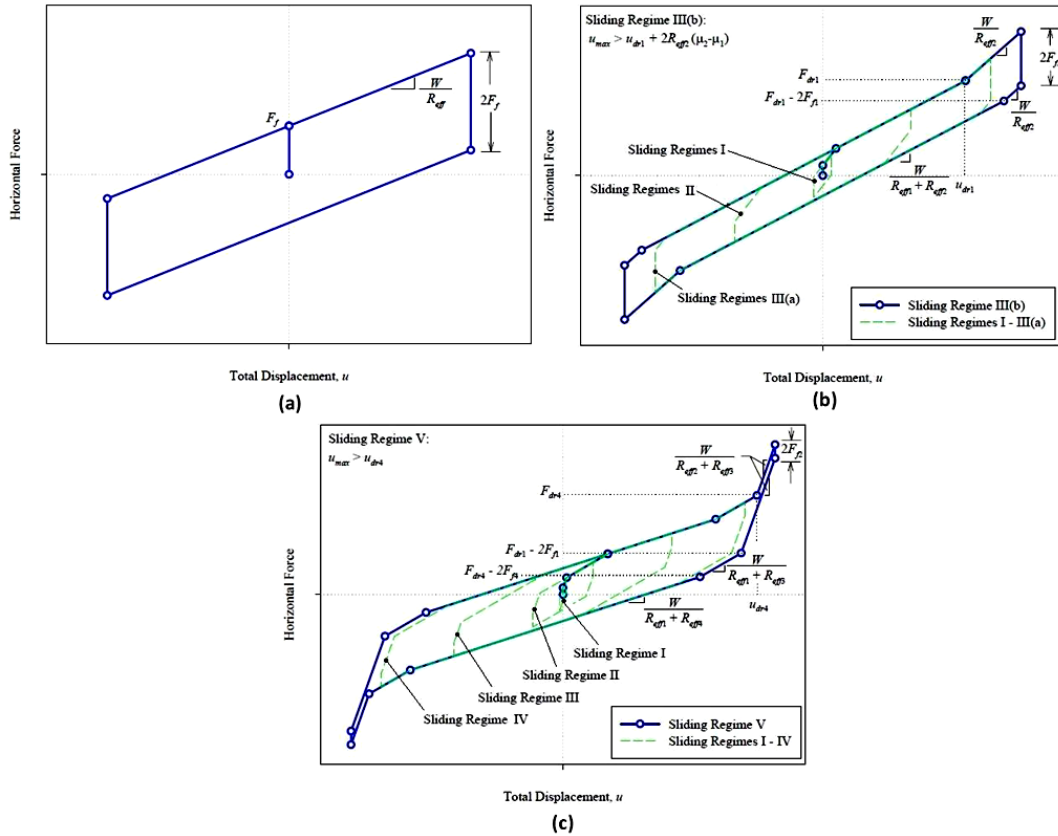


Fig. 3 Hysteresis behavior of: (a) SFP (b) DCFP; and (c) TCFP bearings (Fenz and Constantinou 2008a)

4. Mathematical modeling of TCFP and DCFP Isolators

Fenz and Constantinou (2008a,b) introduced a new approach to model multi-spherical sliding bearing. They combined nonlinear elements in such a way that the whole behavior is experienced.

By employing this approach, two SFP elements are connected in series implemented to simulate a DCFP isolator. Also, by extending this method a TCFP isolator can be modeled by connecting three SFP elements in series. So, the governing equations for TCFP and DCFP isolators are based on SFP equations of motion. The series elements for TCFP and DCFP isolators consist of parallel arrangements of (a) a linear spring, (b) a velocity-dependent perfectly plastic friction element, and (c) a gap element (Fenz and Constantinou 2008a,b).

Despite the fact that a TCFP system is constituted by four sliding surfaces, Fenz and Constantinou present a modified formulation in which the TCFP can be idealized by three independent SFP element connected in series. Because inner sliding surfaces (2 and 3) have similar physical and geometrical properties, they can be modeled by an independent element. The parameters of series elements for TCFP and DCFP isolators were introduced by Fenz and Constantinou (Fenz and Constantinou 2008a,b).

The horizontal force F_i in the isolator can be obtained from the equation of a SFP isolator

motion:

$$F_i = \frac{W}{R_{effi}} u_i + \mu_i W Z_i + F_{ri} \quad (1)$$

u_i : the bearing displacement,

W : the weight of structure,

R_{effi} : the radius of curvature of the sliding surface,

μ_i : the coefficient of friction,

Z_i : a dimensionless hysteretic variable defined in Eq. (2),

F_{ri} : the contact effect with restrainers represented in Eq. (3),

$$\frac{dZ_i}{dt} = \frac{1}{u_{yi}} \{ A_i - |Z_i|^{\eta_i} [\gamma_i \text{sign}(\dot{u}_i Z_i) + \beta_i] \} \dot{u}_i \quad (2)$$

Where \dot{u}_i is the sliding velocity, and $A_i, \eta_i, \gamma_i, \beta_i$ represent dimensionless quantities that control the shape of the hysteresis loop.

$$F_{ri} = k_{ri} (|u_i| - d_i) \text{sign}(u_i) H(|u_i| - d_i) \quad (3)$$

k_{ri} denotes the stiffness after contacting the displacement restrainers which is assigned a large value, and H stands for Heaviside function.

In the most investigations e.g. Fenz and Constantinou (2008a), Morgan and Mahin (2011) and Becker and Mahin (2012) the restrainer is assumed nearly rigid and its stiffness is modified using experimental test. In this research the value of restrainers' stiffness is selected according to the previous investigations (Fenz and Constantinou, 2008a).

5. TCFP, DCFP and SFP Isolators design

It is so important to define appropriate parameters to estimate the overall behavior of isolators. Seismic codes usually propose effective period (T_{eff}) and effective damping (ξ_{eff}) as designing parameters of isolated structures which can be represented by the following equations:

$$T_{eff} = 2\pi \sqrt{\frac{W}{K_{eff} g}}, \quad \xi_{eff} = \frac{1}{2\pi} \left[\frac{E_{loop}}{K_{eff} D^2} \right] \quad (4)$$

In which E_{loop} is the energy dissipation in each cycle of the isolator hysteresis loop, K_{eff} stands for the effective linear stiffness and D shows the target displacement of the isolator.

Many researchers used this method to compare the behavior of different isolators in their investigation. Morgan and Mahin (2011) and Becker and Mahin (2012) designed isolators in such a way that they meet same effective period and damping in a target displacement.

In this investigation, target displacement is assumed as the displacement in the end of sliding regime IV or beginning of sliding regime V of the TCFP, until the whole sliding regime of TCFP is examined. Therefore the comparison was performed in maximum considered earthquake (MCE) level.

K_{eff} and E_{loop} of a SFP isolator can be obtained from following equations:

$$K_{eff} = \left(\frac{\mu}{D} + \frac{1}{R} \right) W \quad (5)$$

$$E_{loop} = 4 \mu DW \quad (6)$$

Based on the previous explanation, K_{eff} and E_{loop} values for other isolators including DCFP and TCFP bearings can be derived by similar equations that can be found in different references such as Becker and Mahin (2013).

The configuration of three types of isolation systems with different isolation period and $\xi_{eff}=15\%$ is listed in Tables 1-3. In design column, the first term represents the type of isolator, the second term stands for effective period and the last one shows the effective damping. Since the seismic responses of different isolator subjected to strong near-field pulses are desired, isolators designed in order to have the capacity of considerable displacement. As it was described previously, dynamic responses of subjected to PGVs varying from 20 to 220 cm/s and pulse periods between 0.5 to 2.5 s are investigated in this research. It is noted that great values of PGV such as 180 and 220 cm/s and pulse periods greater than 2s lead to great displacements in isolators. Therefore, the displacement capacity of isolators is extended in such way ($d=1.5$ m) to accommodate high displacement demands when it is subjected to severe near field pulses. This high capacity permits to the isolators to experience displacement without impact to the restrainers in low values of PGVs and pulse periods and make their performance reasonable when isolators are subjected to high PGVs and pulse periods. It means that exceeding of the maximum displacement of isolators comparing to the displacement capacity is negligible in this investigation.

The isolator configuration was chosen to provide the same effective isolation period and damping in the target displacement. It is possible to find different configuration to set isolator properties which means that the configuration is not unique. Although the design optimization plays an important role in comparing different isolator behavior (especially stiffening part in TCFP), it is beyond this research to optimize and change the design of each isolator for different PGV intervals. Instead, it was attempted to compare some isolators with different specifications such as various period and damping properties. In this study, assigning the appropriate characteristics was done by trial and error method.

The friction specifications of isolators are selected based on the previous investigations. Fenz and Constantinou (2008a) categorized range of possible friction coefficients. In their studies, Low friction is on the order of 0.02 to 0.03, medium friction varies from 0.05 to 0.1 and high friction changes from 0.15 to 0.2. Although friction coefficients between 0.15 and 0.2 are considered very high, it was used for some models in their researches. Morgan and Mahin (2011) have considered friction coefficient of 0.01 to 0.02, 0.05 to 0.08 and 0.1 to 0.2 as low, medium and high values respectively and TCFP with different friction coefficients were analyzed in their studies.

Table 1 Characteristics of SFP isolator

Design	Teff (sec)	Displacement Capacity-D (m)	Effective Radii- R_{eff} (m)	Friction Coefficient- μ
SFP-5-15	5	1.5	8.0	0.058
SFP-4-15	4	1.5	5.3	0.087
SFP-3-15	3	1.5	3.0	0.155

Table 2 Characteristics of DCFP isolator

Design	T _{eff} (sec)	Displacement Capacity-D (m)			Effective Radii-R _{eff} (m)		Friction Coefficient-μ		
		d ₁ =d ₄	d ₂ =d ₃	D(Total)	R _{eff1} =R _{eff4}	R _{eff2} = R _{eff3}	μ ₂ = μ ₃	μ ₁	μ ₄
TCFP-5-15	5	0.65	0.10	1.5	5.5	0.45	0.03	0.065	0.10
TCFP-4-15	4	0.65	0.10	1.5	3.5	0.3	0.05	0.10	0.15
TCFP-3-15	3	0.65	0.10	1.5	1.6	0.2	0.13	0.18	0.2
TCFP-2-15	2	0.65	0.10	1.5	0.6	0.125	0.13	0.18	0.2

6. Analysis of the model

Nearly 3800 nonlinear time history analysis are performed in this study. A common range of isolators with 2, 3, 4 and 5 seconds effective period considering an extensive range of effective damping consist of 10, 15, 20, 25 and 30 percent are investigated. To find out the effects of superstructure, 3 types of superstructures with 0.2, 0.5 and 0.8 s period, are considered.

In this study, the impacts of Peak Ground Velocity (PGV) of the near-field pulses on seismic responses of different base-isolated structures are contemplated. To fulfill this aim, different pulses are selected and imposed to the structural models. In the near-field ground motions both the fling step and the forward directivity pulses, PGV is a determinant parameter. It is demonstrated that the PGV has significant effects on seismic responses of structures subjected to the near-field ground motions in the previous studies. (Kalkan and Kunnath, 2006) In this investigation, a wide range of the near-field PGV pulses are selected consist of 20, 60, 100, 140, 180 and 220 cm/s. To avoid the effects of pulse period (T_p), only short values of pulse periods are considered. The period of applied pulses either for the forward directivity or for the fling step is assumed 0.5, 1, 1.5, 2 and 2.5 seconds (Kalkan and Kunnath 2006, Khoshnoudian and Ahmadi 2013).

Superstructure is modeled as a SDOF system mounted on different friction isolators. The series model for DCFP and TCFP isolators which were introduced by Fenz and Constantinou are employed to idealize these isolators (Fenz and Constantinou 2008a,b). The above-mentioned pulses are imposed on the structures and through nonlinear time history analysis, different responses are extracted. Maximum isolator displacement and maximum base shear of superstructure are selected as two prominent isolated-structure responses. As it will be presented in next section, drift and absolute acceleration have a similar trend to the base shear; therefore, base shear can be a good representative of the other responses.

7. Effects of main parameters on seismic responses of TCFP bearing

7.1 Near-fault pulse and its PGV

The bearing displacement and the normalized base shear as main responses are depicted in

Figs. 4 and 5. In these Figs, the effects of PGV variation of the forward directivity and the fling step pulses on seismic responses of TCFP isolator with effective isolation period of 4 s are illustrated.

According to Fig. 4, isolator displacement in the forward directivity pulses is greater than in fling step pulses to a large extent for a constant PGV. For example, the displacement of a TCFP isolator with effective period of 4 seconds and damping ratio of 15% is 103cm under a fling pulse with $T_p=2.5s$ and $PGV=220$ cm/s. The same isolator shows 183cm displacement under a similar forward directivity pulse. As it is demonstrated in Fig. 2, the forward directivity has a pulse period 1.5 times as much as the fling step pulse. It means that the structure imposes to the excitation with longer time duration under the forward directivity pulses. According to Fig. 2, comparing the forward directivity and the fling step pulses with equal PGVs, the forward directivity peak ground acceleration (PGA) which is occurred in $0.75T_p$, is two times of the fling step pulse PGA. Since ground velocity time history is the integration of the ground acceleration pulse, raising the pulse PGV leads to increasing the pulse PGA.

Therefore, it is reasonable that the forward directivity pulses lead to greater responses e.g. isolator displacement in comparison to the fling step ones. The similar trend can be seen in Fig. 5 for the normalized base shear. The forward directivity pulses cause greater base shear in comparison to the fling step ones. The normalized base shear of a TCFP isolator with effective period of 4s and damping ratio of 15% is 0.27 and more than 1 under fling step and forward directivity pulses, respectively. The main reason can be described similar to what was discussed previously.

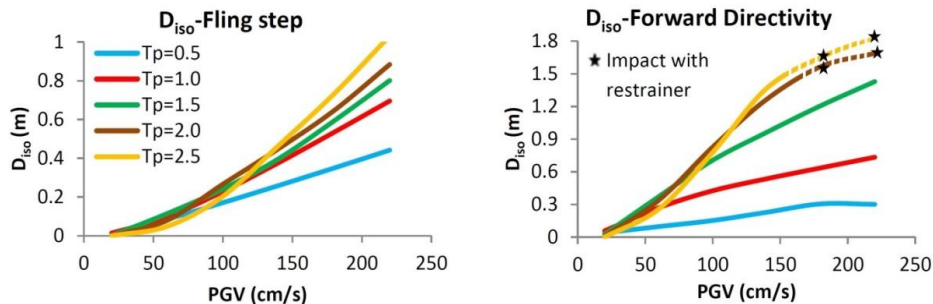


Fig. 4 Isolator displacement for TCFP isolators ($T_{eff}=4s$, $T_s=0.5s$ and $\xi_{eff}=15\%$)

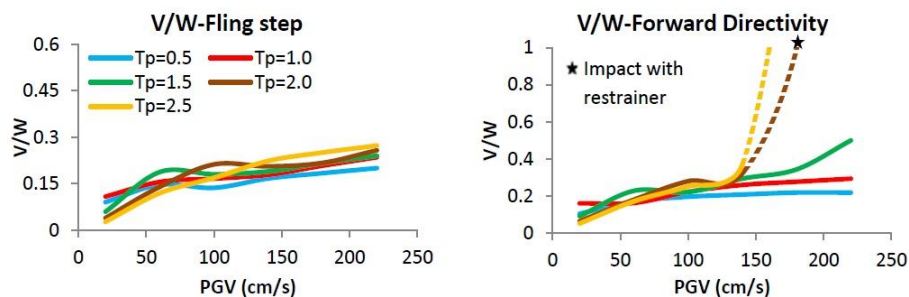


Fig. 5 Normalized base shear for TCFP isolators ($T_{eff}=4s$, $T_s=0.5s$ and $\xi_{eff}=15\%$)

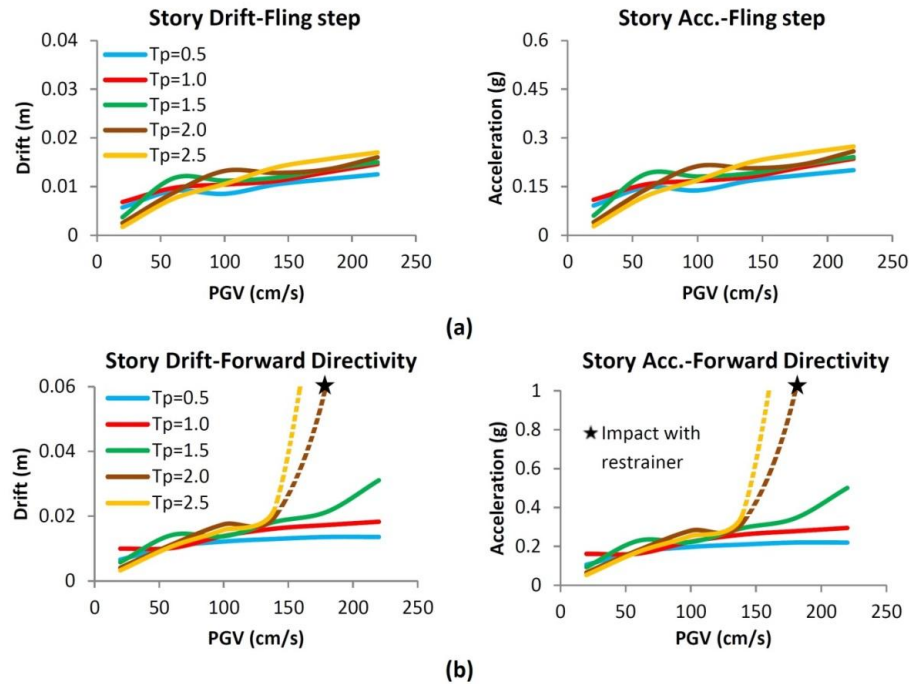


Fig. 6 Story drift and acceleration of TCFP isolators ($T_{eff}=4s$, $T_s=0.5s$ and $\xi_{eff}=15\%$) in a)Fling step b)Forward directivity pulses

According to Figs. 4 and 5, either the isolator displacement or the normalized base shear is rising when the PGV increases. The rate of this increase is not the same for different pulse periods. This rate is great for pulses with longer periods and decreases when the pulse period becomes shorter. For a TCFP isolator subjected to the forward directivity pulses (Fig. 4), isolator displacement under a pulse with $T_p=0.5$ second is changing from 3 cm for PGV=20 cm/s to 30 cm for PGV=220 cm/s, while the displacement for the same isolator under a pulse with $T_p=2.5$ second varies from less than 1 cm for PGV=20 cm/s to 184 cm for PGV=220 cm/s. It seems reasonable that increasing both the PGV and the T_p of a ground motion ascend the effect of excitation on the structure. As it was discussed before, It is understandable that increasing both PGA and T_p , intensify the responses of the structure. So, as it can be seen in Fig. 4, the rate of rising in isolator displacement in pulses with longer pulse periods is more than shorter period pulses.

Fig. 5 shows the variation of normalized base shear versus the variation of PGV for the forward directivity and the fling step pulses. In some cases, there is a huge rising in values of the normalized base shear subjected to the forward directivity pulses. Comparing to the Fig. 4, (isolator displacements), it is revealed that in these cases the isolators reach to its displacement capacity (1.5 m) where the slider meets the isolator restrainers. Therefore, the superstructure experiences the effect of this impact which exert a great acceleration and base shear through the structure. Investigation of this impact is beyond the scope of this study and needs another research in order to scrutinize elaborately. The displacement and base shear values related to the models that experience the impact, are marked with “star” in Figs 4 and 5 respectively. It is noted that

these results presented with dash-line are not reliable.

The story drift and acceleration of superstructure is depicted in Fig. 6. The effect of PGV variations of fling step and forward directivity on a TCFP isolator with effective period of 4 sec is indicated in the Fig. Comparing the trend of story drift and acceleration with the base shear that are illustrated in Fig. 5, reveals that these three responses i.e. story drift, story acceleration and base shear varies in similar patterns. Therefore, hereafter only the displacement and base shear diagrams of different isolator will be presented.

7.2 Isolator effective period (T_{eff})

The effects of isolator effective period on the bearing displacement and the base shear are illustrated in Figs 7 and 8. Fig. 7 shows that increasing in the effective isolation period rises bearing displacement. Rising the effective period of isolator from 3s to 5s causes the increase of a TCFP isolator displacement from 43cm to 125cm subjected to a fling step pulse with $T_p=2.5$ s and $PGV=220$ cm/s. A similar trend can be seen using forward directivity pulses as well. As isolators with longer effective period have less effective stiffness, they experience larger displacement in comparison to the isolators with shorter period. This effect on base shear is vice-versa. In this case, the normalized base shear decreases from 0.37 to 0.2. It is reasonable that isolators with longer

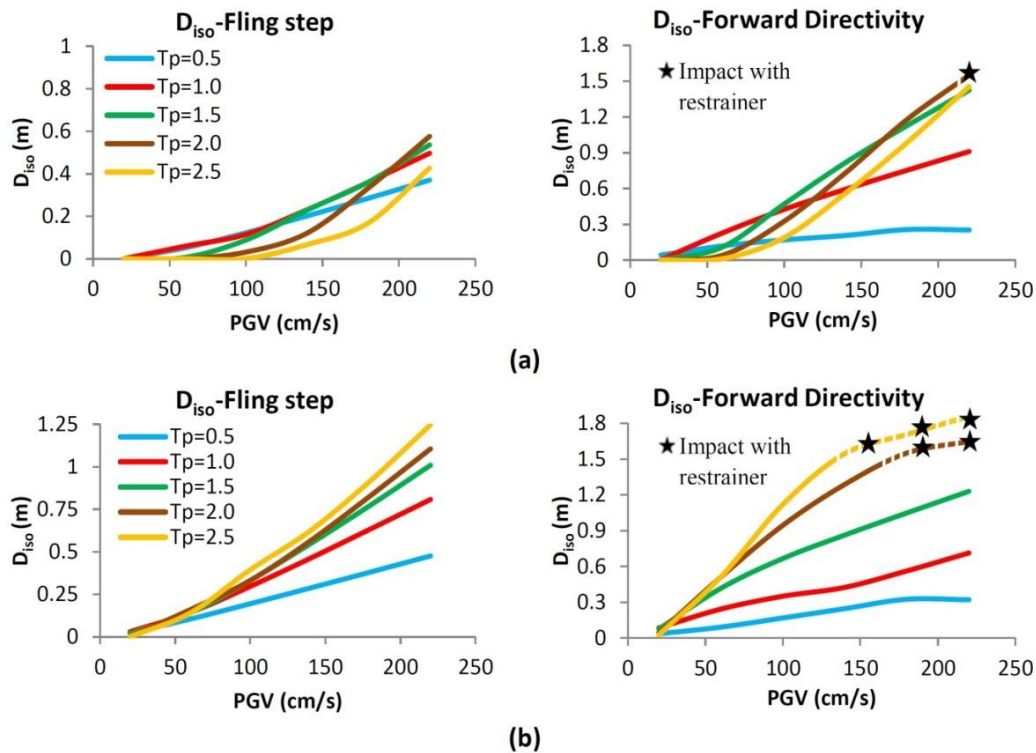


Fig. 7 Isolator displacement for TCFP isolators, a) $T_{eff}=3$ sec, b) $T_{eff}=5$ sec ($T_s=0.5$ s and $\xi_{eff}=15\%$)

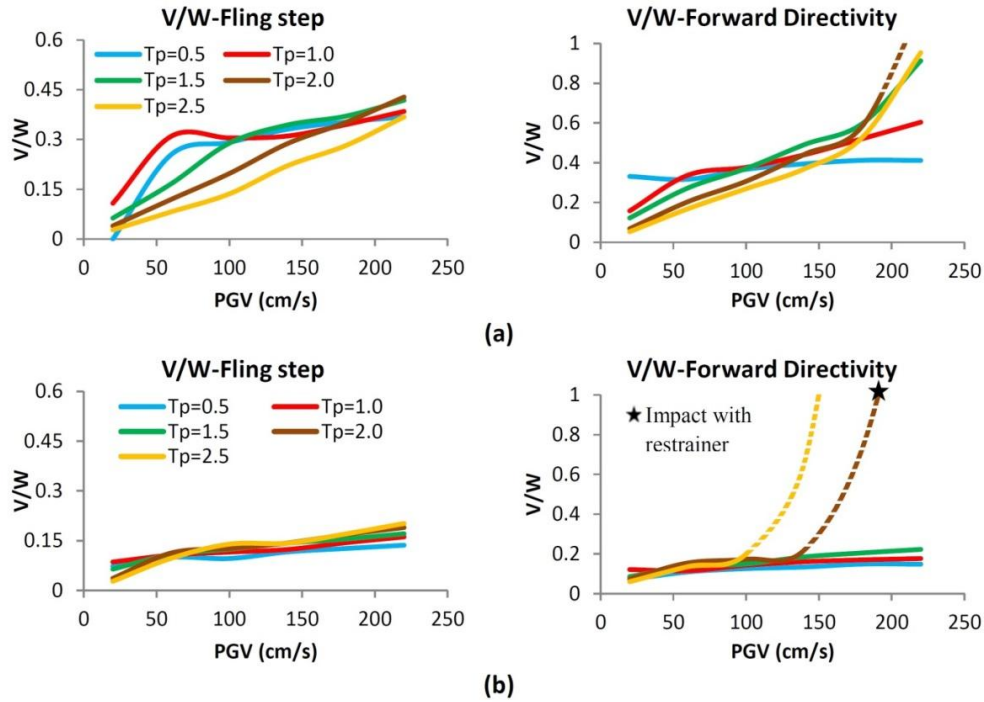


Fig. 8 Normalized base shear for TCFP isolators, a) $T_{\text{eff}}=3$ sec, b) $T_{\text{eff}}=5$ sec ($T_s=0.5$ s and $\xi_{\text{eff}}=15\%$)

period experience smaller base shear due to its less effective stiffness. Obviously in Figs 7 and 8, the forward directivity responses overcome the fling step ones. Furthermore, the seismic responses rise with increasing of the ground motion PGV. The rate of increasing in isolator displacement and base shear is not equal for different pulse periods. The greater increasing rate belongs to pulses with longer periods. The reason is the same as discussed previously for Fig. 4.

7.3 Isolator damping (ξ_{eff})

The effect of isolation damping on isolator displacement and normalized base shear is demonstrated in Figs 9 and 10. For a TCFP isolator with $T_{\text{eff}}=4$ s considering a wide range of effective damping 10, 20 and 30% damping are selected to investigate this effect. As Figs 9 and 10 reveals, rising in isolator damping plays an essential role in decreasing the isolator displacement, while the decrease is not remarkable in normalized base shear. As an example increasing the isolator damping from 10% to 30% leads to a decrease in TCFP displacement from 128cm to 41cm subjected to a fling step pulse with $T_p=2.5$ s and $\text{PGV}=220$ cm/s. This decrease is calculated from 0.32 to 0.3 in normalized base shear for the same cases. The decline of displacement and base shear are more remarkable in the fling step pulses. The reason is that the isolator displacement in most cases subjected to the forward directivity pulses is more than 1.5 m, the displacement capacity of the bearing. It means that the bearing experiences the regime 5 of its backbone curve. Although increasing the damping decreases the maximum displacement, its effect is not remarkable when the isolated-structure is subjected to strong ground motions. “Star” marks and dash-lines are used for indicating the values in models which experience the restrainer’s impact as well as the previous sections.

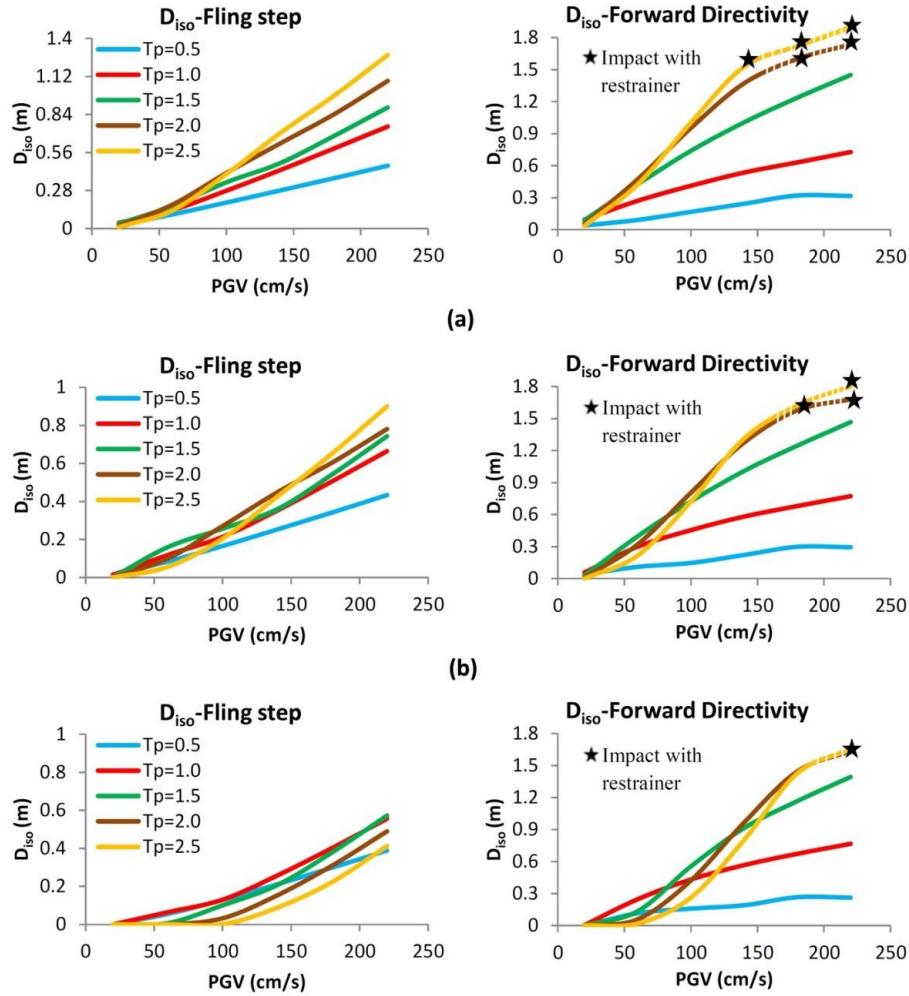


Fig. 9 Isolator displacement for TCFP isolators, a) $\xi_{\text{eff}}=10\%$, b) $\xi_{\text{eff}}=20\%$, c) $\xi_{\text{eff}}=30\%$ ($T_{\text{eff}}=4\text{s}$, $T_s=0.5\text{s}$)

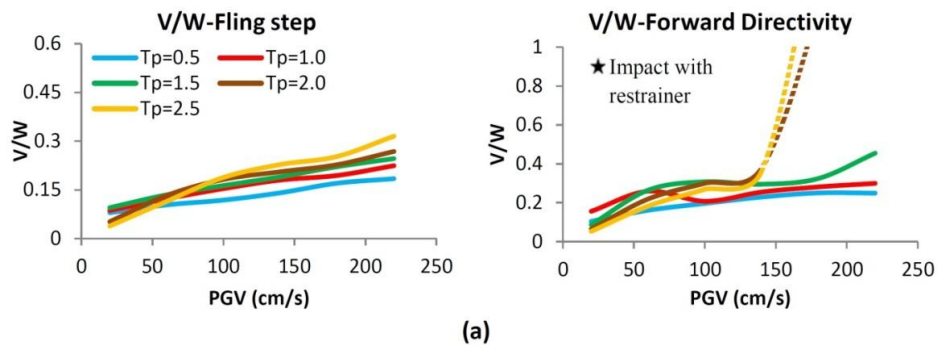


Fig. 10 Normalized base shear for TCFP isolators, a) $\xi_{\text{eff}}=10\%$, b) $\xi_{\text{eff}}=20\%$, c) $\xi_{\text{eff}}=30\%$ ($T_{\text{eff}}=4\text{s}$, $T_s=0.5\text{s}$)

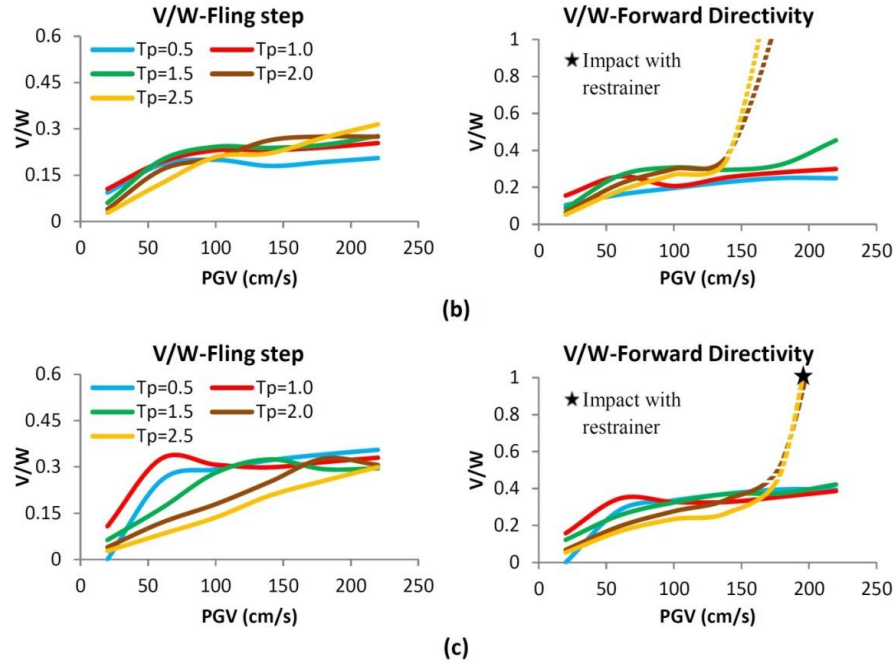


Fig. 10 Continued

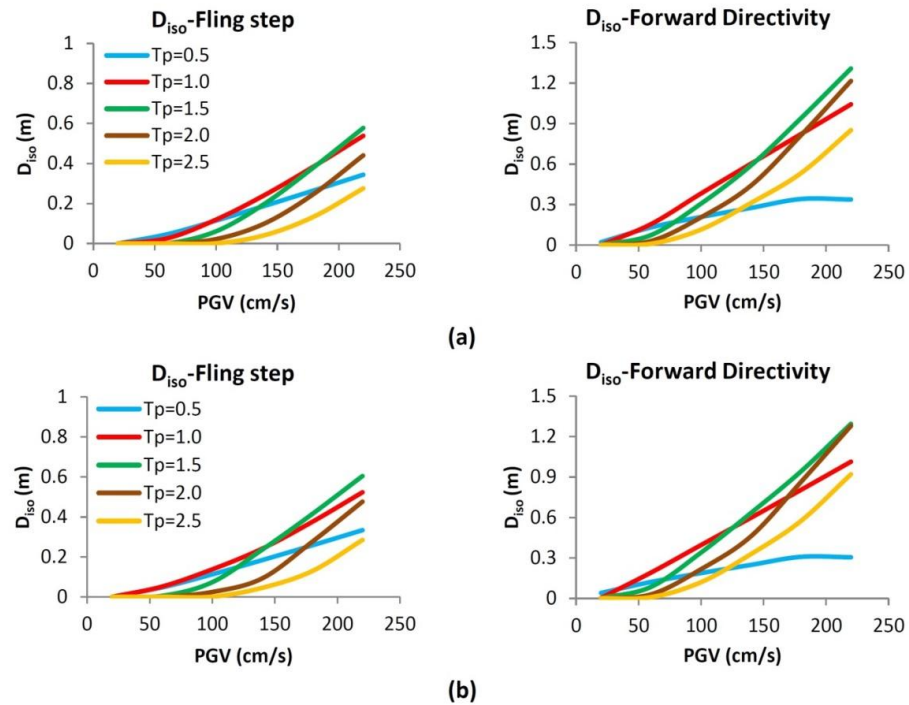
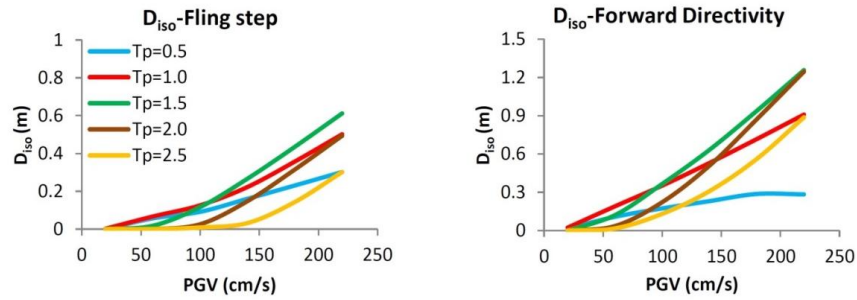


Fig. 11 Isolator displacement for TCFP isolators, a) $T_s = 0.2$ sec, b) $T_s = 0.5$ sec c) $T_s = 0.8$ sec ($T_{eff} = 2s$, $\xi_{eff} = 15\%$)



(c)
Fig. 11 Continued

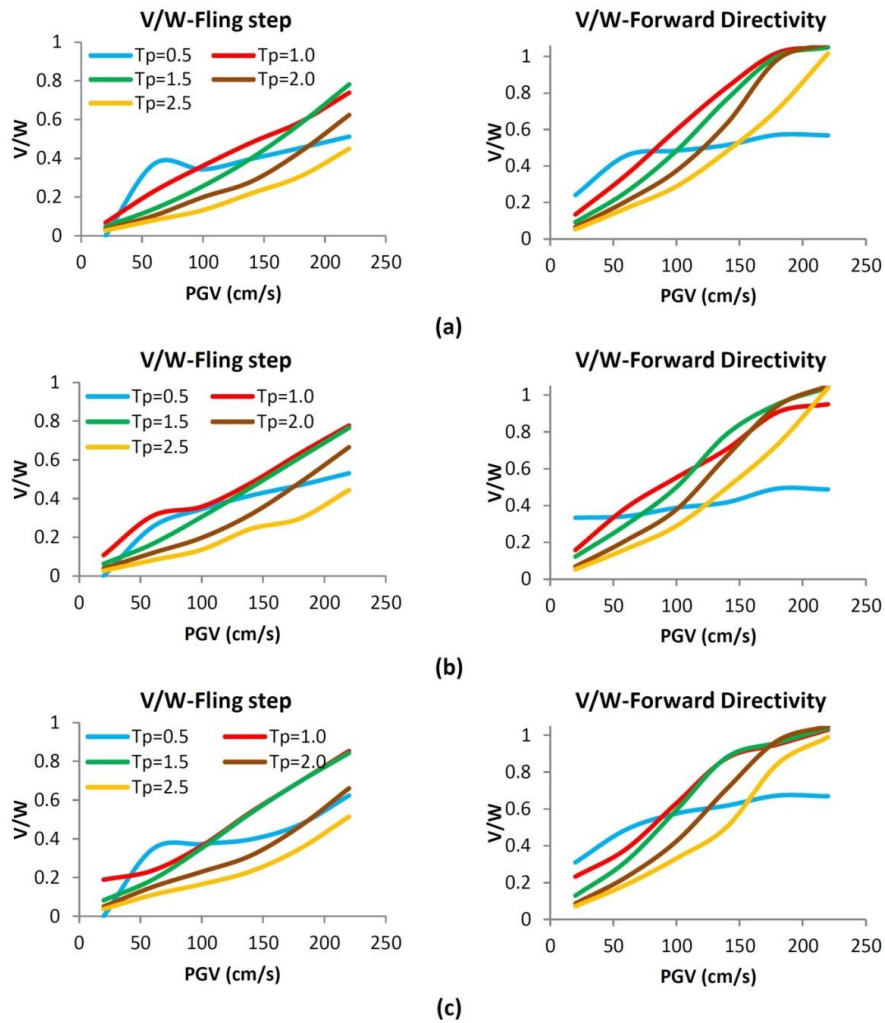


Fig. 12 Normalized base shear for TCFP isolators, a) $T_s=0.2$ sec , b) $T_s=0.5$ sec c) $T_s=0.8$ sec ($T_{eff}=2s$, $\xi_{eff}=15\%$)

7.4 Superstructure period (T_s)

Another parametric study is performed to reveal the role of superstructure period in structure responses. Figs 11 and 12 exhibit the results for different superstructures with $T_s = 0.2, 0.5$ and 0.8 sec mounted on a TCFP isolator with $T_{eff} = 2$ s and $\xi_{eff} = 15\%$. The TCFP isolator with minimum effective period (2 sec) is selected in order to better investigate the effect of superstructure period. As it was discussed previously the effect of isolators with shorter effective periods on the seismic responses of isolated structure is less than longer-period ones.

For instance, increasing the superstructure period from 0.2 s to 0.8 s increases the TCFP displacement from 27 cm to 30 cm subjected to fling step pulse with $PGV = 220$ cm/s and pulse period of 2.5 sec. In this case, the normalized base shear is enhanced from 0.45 to 0.51 . For a similar forward directivity pulse, the displacement is increased from 85 cm to 89 cm. The results demonstrate that the superstructure period has no considerable effect on seismic responses. Generally, the trend of variation shows that the forward directivity effects are dominant comparing to the fling step ones.

8. Comparison of SFP, DCFP and TCFP Isolators responses

To investigate the effect of PGV of near-field pulses on the seismic responses of structures isolated with SFP and DCFP isolators, the isolator displacements are presented in Figs 13 and 14. Fig. 13 shows the isolator displacements of SFP and DCFP bearings with $3, 4$ and 5 sec effective periods subjected to fling step pulses. Comparing with Fig. 7 reveals that similar patterns govern the behavior of all three kinds of friction isolators i.e. SFP, DCFP and TCFP. For example in a fling step pulse with $T_p = 2.5$ s and $PGV = 220$ cm/s, increasing the T_{eff} of isolator from 3 sec to 5 sec increases the isolator displacement from 54 cm to 142 cm in SFP bearing and from 57 cm to 140 cm in DCFP one.

Fig. 14 demonstrated that increasing the effective damping play an important role in decreasing the isolator displacement in SFP and DCFP isolators as well as TCFP one, which was discussed previously in Fig. 9. However, the results of forward directivity pulses as well as structure base shear are negligible here.

To compare the SFP, DCFP and TCFP isolators' responses in more detail, the displacements and base shear of different isolated structures subjected to the fling step and the forward directivity pulses with $T_{eff} = 5$ s and $\xi_{eff} = 15\%$ are illustrated in Figs 15 and 16. For contraction, only the results of PGV values more than 100 cm/s for $T_p = 2$ s and 2.5 s are presented herein.

Fig. 15 reveals that for pulses with T_p equal 2 seconds, TCFP isolator reduces the displacement in the fling step pulses to some extent; for instance, the TCFP isolator has decreased the displacement in 2.5 s pulse up to 12% comparing to SFP one. Meanwhile implementing the DCFP isolator is not very efficient. In addition, none of the multi-spherical isolators i.e. DCFP and TCFP can reduce the bearing displacement when they are subjected to forward directivity pulses. It can be expected that in forward directivity pulsed with 2 s and 2.5 s period, due to the severity of the earthquake, all three types of bearing will reach to their displacement capacity. Three types of isolators were designed for total displacement capacity of 1.5 m; therefore, the isolator displacement is the same for all of them because they reached to their maximum designed displacement capacity. As an example, in 2.5 s period pulse with PGV equal to 180 cm/s, the

bearing displacement in forward directivity pulse is more than 1.5m, the isolator displacement capacity, in all three bearings. This means that DCFP and TCFP isolators cannot decrease the structure displacement in comparison with SFP one when a strong near-field earthquake occurs. The displacements of these three isolators can be seen in Fig. 17 as well. This Fig. demonstrates the hysteresis loops of different isolators subjected to either the fling step or the forward directivity pulses. In this Fig., the effect of impact between slider and isolator end restrainers where the isolator reaches to its total displacement capacity can be seen. As it is clearly illustrated in this Fig., in forward directivity pulse with $T_p=2.5$ s and $PGV=180$ cm/s the slider parts reaches to the restrainer edges, where the displacement in all three bearings is limited to 1.5m. Consequently, SFP, DCFP and TCFP isolators have the same displacement, so the comparison of isolator displacements would be meaningless beyond the bearing capacity.

Fig. 17, denotes that the DCFP can reduce the base shear of superstructure to some extent. As an example the TCFP isolator decreases the base shear up to 30% and 45% comparing to SFP and DCFP bearings assuming $T_p=2.5$ sec and subjected to fling step pulses. In forward directivity pulses, the TCFP base shear is less than SFP and DCFP as well, but the differences are not as remarkable as fling step pulses. The reason can be seen in Fig. 17 where the base-isolated structure subjected to the forward directivity pulses with great values of PGV. In this case, the bearing displacement reaches to its capacity displacement and due to the impact between slider and restrainer the normalized base shear is more than 1. Therefore, all three types of isolators have the same base shear.

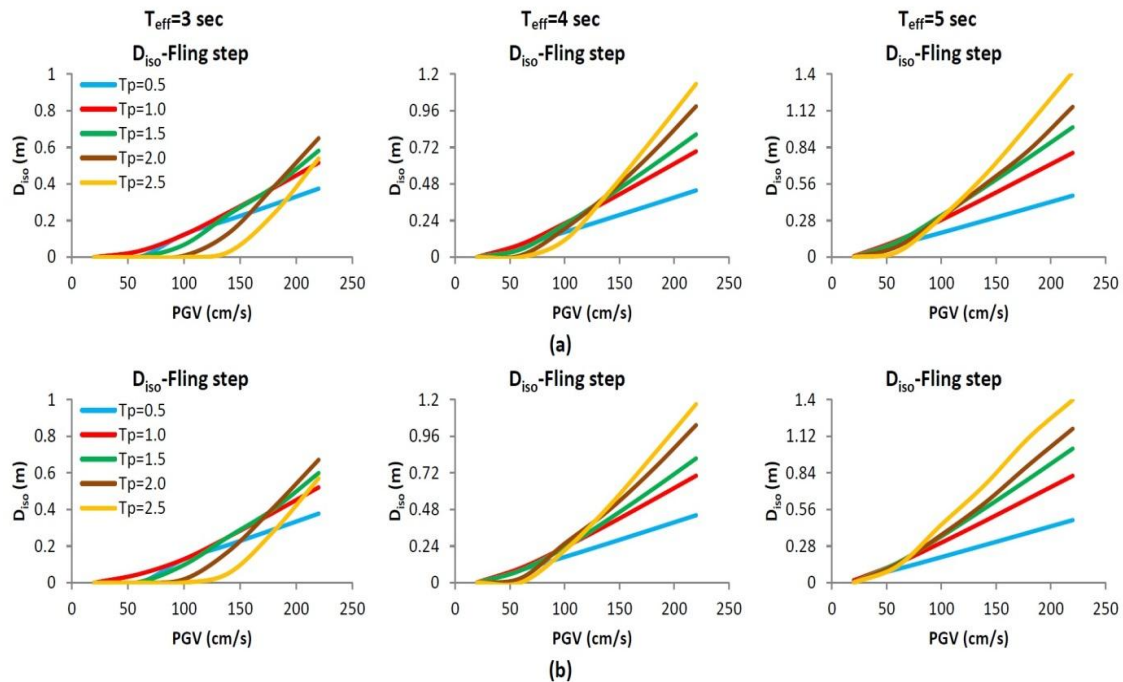


Fig. 13 Isolator displacement in fling step pulses a)SFP b)DCFP isolators with different periods ($T_s=0.5$ s, $\xi_{eff}=15\%$)

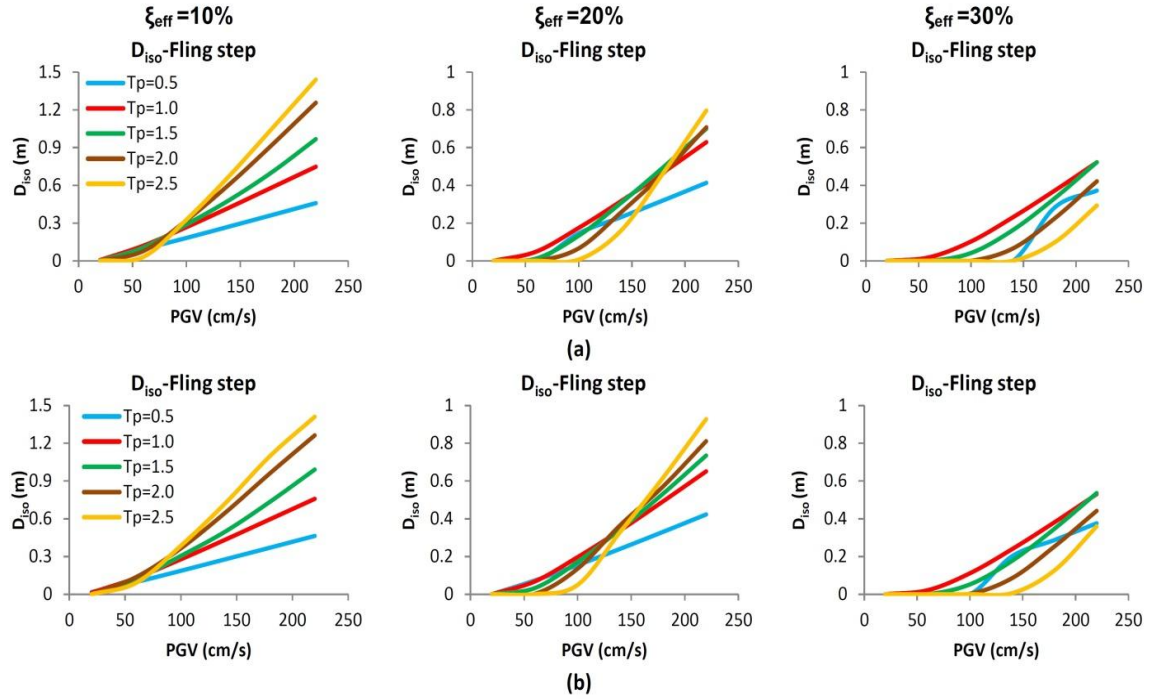


Fig. 14 Isolator displacement in fling step pulses a)SFP b)DCFP isolators with different dampings ($T_s=0.5s$, $\xi_{eff}=15\%$)

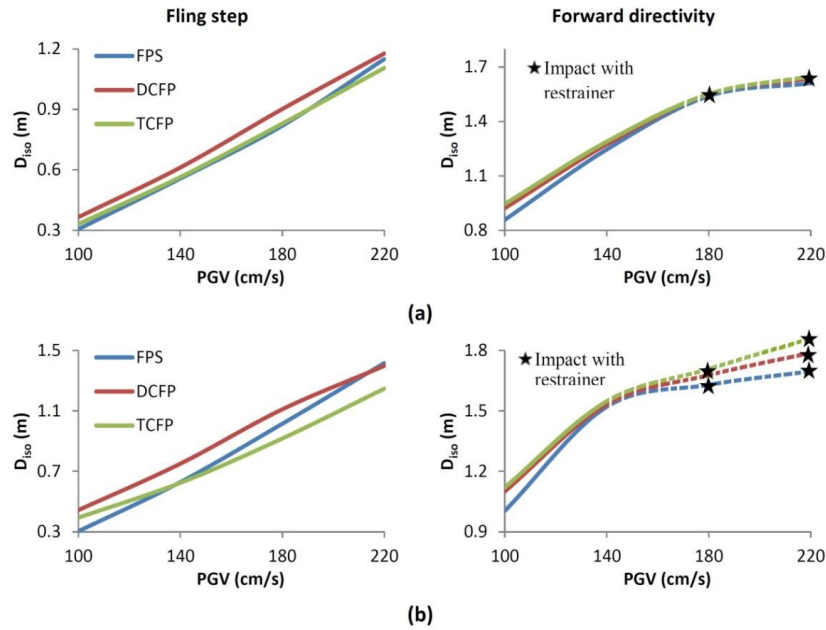


Fig. 15 Displacement of isolated structures subjected to fling step and forward directivity pulses, a) $T_p=2$ sec , b) $T_p=2.5$ sec ($T_{eff}=5s$, $\xi_{eff}=15\%$ and $T_s=0.5s$)

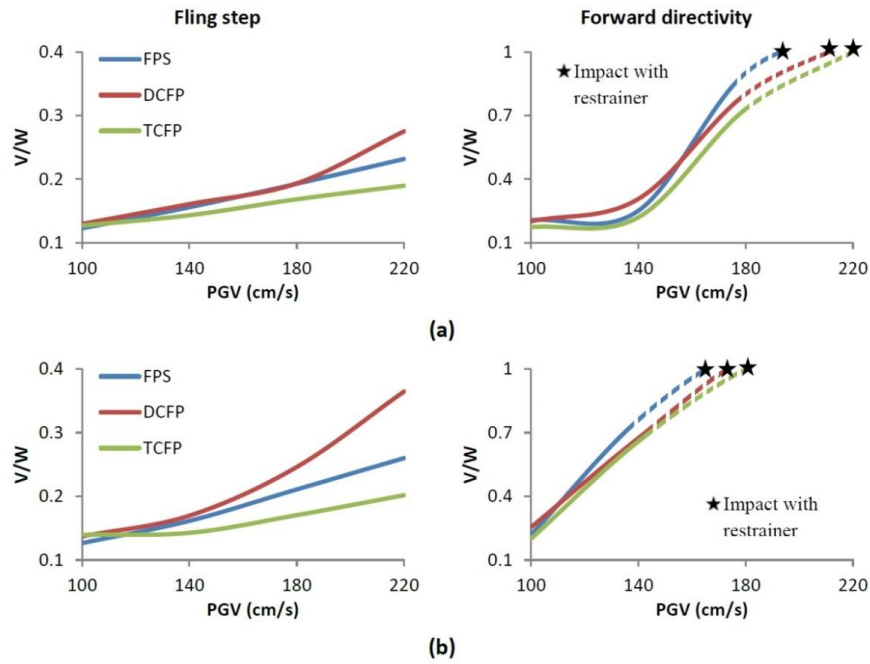


Fig. 16 Normalized base shear of isolated structures subjected to fling step and forward directivity pulses, a) $T_p=2$ sec, b) $T_p=2.5$ sec ($T_{eff}=5s$, $\xi_{eff}=15\%$ and $T_s=0.5s$)

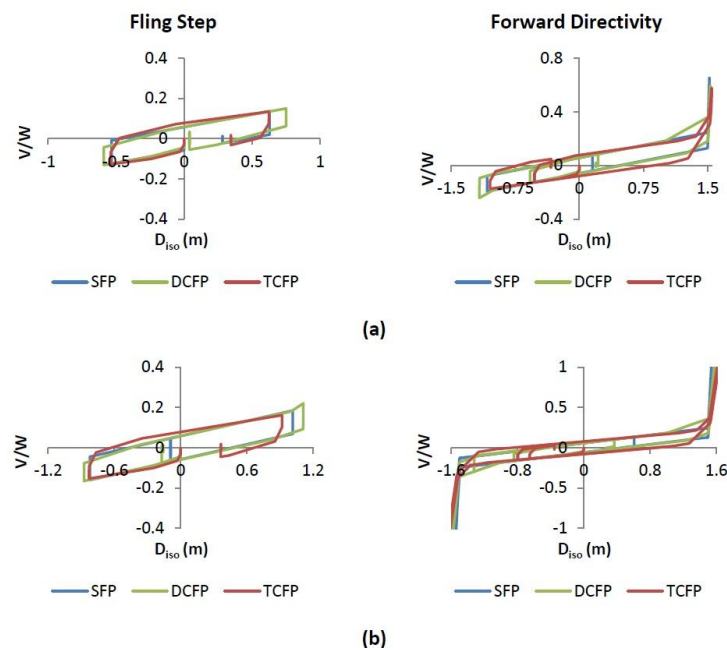


Fig. 17 Hysteresis diagrams of different isolators, a) $PGV=140$ cm/s, b) $PGV=180$ cm/s ($T_{eff}=5s$, $\xi_{eff}=15\%$ and $T_s=0.5s$)

9. Conclusion

This investigation has been conducted in order to emphasize the effects of Peak Ground Velocity (PGV) of the near-field pulses on responses of base-isolated structures employing different types of friction isolators consist of SFP, DCFP and TCFP bearings. Different superstructures mounted on an extensive range of isolators with various effective periods and effective damping subjected to two well-known mathematical near-field pulses, the forward directivity and the fling step, are considered in this paper. The superstructure and isolators are idealized using linear and nonlinear behaviours respectively and subjected to forward directivity and fling step pulses. Period of applied pulses varies from 0.5 to 2.5 second considering PGV changes from 40 to 220 cm/s. The results of this investigation can be summarized as:

- TCFP isolator displacement and superstructure base shear subjected to the forward directivity pulses are greater than similar responses using the fling step ones. As an example, in bearings with $T_{eff}=4$ sec, forward directivity displacements are 80 percent more than fling step ones. But this value is about 50 percent for $T_{eff}=5$ sec. The base shear of forward directivity pulse is 50 and 40 percent greater than fling step pulse respectively employing bearings with effective period isolators of 4 and 5 seconds. The effects of forward directivity pluses are more hazardous than the fling step pluses and should be considered in practical design too.
- Increasing the ground motion velocity (PGV) causes the structure responses to rise up. This increase happens both in the forward directivity and the fling step pulses. In pulses with longer periods this rising becomes more in comparison with the shorter one. As an example, isolators with effective period of 5 sec subjected to forward directivity pulses, the rate of displacement becomes 8 times when the pulse period increases from $T_p=0.5s$ to $T_p=2.5s$. A similar trend can be demonstrated in base shear results as well. As the pulse PGV is the integration of the time history of pulse acceleration, increasing the pulse PGV is equal to raising its PGA. While increasing both PGV and T_p of a pulse, it is obvious that its effect on the structure intensifies.
- Increasing the isolator period rises its displacement while it decreases the superstructure base shear and consequently the absolute acceleration of superstructure and drift enhancing of the effective period of TCFP isolated structures from 3s to 5s increases the displacement up to 190 percent and decreases the base shear up to 45 percent.
- The superstructure properties have not any considerable effect on seismic responses, while the isolator effective damping can play an important role in controlling the isolator displacement.
- TCFP isolators can reduce the bearing displacement and superstructure base shear in comparison with the DCFP and SFP isolators subjected to fling step pulses with long periods and great PGVs. However, they are not efficient in controlling the bearing displacements considering forward directivity ones. Results of this investigation shows that this decrease for TCFP isolators is up to 12 percent in bearing displacement and 30 percent in base shear in comparison with SFP one. DCFP isolators do not show any priority comparing to SFP when subjected to the near field pulses.
- It is noted that the above conclusions are reliable only for friction isolators with effective periods of 2 sec to 5 sec and effective damping of 10% to 30%. The generalization of the results to any other kind of isolation system or friction isolators beyond the scope of this paper needs more investigation.

References

- Agrawal, A.K. and He, W.L. (2002) "A closed-form approximation of near-fault ground motion pulses for flexible structures", Proceedings of the 15th ASCE engineering mechanics conference, Columbia University, New York, NY, USA.
- Alavi, B. and Krawinkler, H. (2004), "Behavior of Moment-resisting Frame Structures Subjected to Near-Field Ground Motions", *Earthq. Eng. Struct. Dyn.*, **33**, 687-706.
- Anderson, J. and Bertero, V. (1978), "Uncertainties in establishing design earthquake", *ASCE, J. Struct. Eng.*, **113**(8), 1709-1724.
- Baker, J.W. (2007), "Quantitative classification of near-fault ground motions using wavelet analysis", *Bull. Seismol. Soc. Am.*, **97**(5), 1486-1501.
- Becker, T.C. and Mahin, S.A. (2012), "Experimental and Analytical Study of the Bi-directional Behavior of the Triple Friction Pendulum Isolator", *Earthq. Eng. Struct. Dyn.*, **41**, 355-373.
- Becker, T.C. and Mahin, S.A. (2013), "Approximating Peak Responses in Seismically Isolated Buildings Using Generalized Modal Analysis", *Earthq. Eng. Struct. Dyn.*, **42**, 1807-1825.
- Bertero, V., Mahin, S. and Herrera, R.A. (1978), "Seismic design implication of near-fault San Fernando earthquake records", *Earthq. Eng. Struct. Dyn.*, **6**, 31-42.
- Constantinou, M.C., Tsopelas, P., Kim, Y.S. and Okamoto, S. (1993), *NCEER-Taisei Corporation Research Program on Sliding Seismic Isolation Systems for Bridges: Experimental and Analytical Study of a Friction Pendulum System (SFP)*, Technical Report NCEER-93-0020, National Center for Earthquake Engineering Research, State University of New York at Buffalo, Buffalo, NY, USA.
- Dao, N.D., Ryan, K.L., Sao, E. and Sasaki, T. (2013), "Predicting the displacement of triple pendulum™ bearings in a full-scale shaking experiment using a three-dimensional element", *Earthq. Eng. Struct. Dyn.*, **42**, 1677-1695.
- Fadi, F. and Constantinou, M.C. (2009), "Evaluation of Simplified Methods for Analysis for structures with Triple Friction Pendulum isolators", *Earthq. Eng. Struct. Dyn.*, **39**, 5-22.
- Fenz, D.M. and Constantinou, M.C. (2006), "Behavior of the double concave Friction Pendulum bearing", *Earthq. Eng. Struct. Dyn.*, **35**, 1403-1424.
- Fenz, D. and Constantinou, M.C. (2008), *Mechanical Behavior of Multi-Spherical Sliding Bearings*, Report No. MCEER-08/0007, MCEER, Buffalo, NY, USA.
- Fenz, D. and Constantinou, M.C. (2008), "Modeling triple friction pendulum bearings for response history analysis", *Earthq. Spectra*, **24**, 1011-1028.
- Fenz, D. and Constantinou, M.C. (2008), "Spherical Sliding Isolation Bearings with Adaptive Behaviors: Theory", *Earthq. Eng. Struct. Dyn.*, **37**, 163-183.
- Fenz, D. and Constantinou, M.C. (2008), "Spherical Sliding Isolation Bearings with Adaptive Behaviors: Experimental Verification", *Earthq. Eng. Struct. Dyn.*, **37**, 185-205.
- Hyakuda T., Saito, K., Matsushita, T., Tanaka, N., Yoneki, S., Yasuda, M., Miyazaki, M., Suzuki, A. and Sawada, T. (2001), "The structural design and earthquake observation of a seismic isolation bearing using friction pendulum system", 7th international seminar on seismic isolation, passive energy dissipation and active control of vibration of structure, Assisi, Italy, October.
- Kalkan, E. and Kunnath, S.K. (2006), "Effects of Fling Step and Forward Directivity on Seismic Response of Buildings", *Earthq. Spectra*, **22**, 367-390.
- Khoshnoudian, F. and Rabie, M. (2010), "Earthquake response of Double Concave Friction Pendulum Base-isolated Structures Considering Vertical Component of Earthquake", *Adv. Struct. Eng.*, **13**, 1-14.
- Khoshnoudian, F. and Hemmati, A. (2011), "Seismic response of Base-isolated Structures Using DCFP Bearings with Tri-Linear and Bi-Linear Behaviors" 12th Asia-Pacific Conference on Structural Engineering and Construction, *Procedia Engineering*, **14**, 3027-3035.
- Khoshnoudian, F. and Ahmadi, E. (2013), "Effects of pulse period of near-field ground motions on the seismic demands of soil-MDOF structure systems using mathematical pulse models", *Earthq. Eng. Struct. Dyn.*, **42**, 1565-1582.

- Kim, Y.S. and Yun, C.B. (2007), "Seismic response characteristics of bridges using double concave friction pendulum bearings with tri-linear behavior", *Eng. Struct.*, **29**, 82-93.
- Krawinkler, H. and Alavi, B. (1998), "Development of an improved design procedure for near-fault ground motions", SMIP 98 seminar on utilization of strong motion data, Oakland, CA, USA.
- Loghman, V., Khosnoudian, F. and Banazadeh, M. (2013), "Effects of vertical component of earthquake on seismic responses of triple concave friction pendulum base-isolated structures", *J. Vib. Control*, DOI: 10.1177/1077546313503359.
- Mahin, S., Bertero, V., Chopra, A.K. and Collins, R. (1976), *Response of the Olive View hospital main building during the SanFernando Earthquake*, Earthquake Engineering Research Center (EERC), Report No. 76/22.1976, University of California (UCB), Berkeley, CA, USA.
- Mahin, S.A. and Bertero, V. (1981), "An evaluation of inelastic seismic design spectra", *ASCE, J. Struct. Eng.*, **107**, 1777-1795.
- Morgan, T. and Mahin, S.A. (2010), "Achieving reliable seismic performance enhancement using multi-stage friction pendulum isolators", *Earthq. Eng. Struct. Dyn.*, **39**, 1443-1461.
- Morgan, T.A. and Mahin, S.A. (2011), *The Use of Base Isolation Systems to Achieve Complex Seismic Performance Objectives*, Report No. PEER-2011/06, Pacific Earthquake Engineering Research Center (PEER), Berkeley, CA, USA.
- Sasani, M. and Bertero, V. (2000), "Importance of severe pulse-type ground motion in performance-based engineering: historical and critical review", *Proceedings of the 12th world conference on earthquake engineering*, New Zealand.
- Somerville, P. (1998), "Development of an improved representation of near-fault ground motions", SMIP98 Proceedings, Seminar on Utilization of Strong-Motion Data, Oakland, California Division of Mines and Geology, Sacramento, CA, USA.
- Takewaki, I., Kanamori, M., Yoshitomia, S. and Tsuji, M. (2013), "New experimental system for base-isolated structures with various dampers and limit aspect ratio", *Earthq. Struct., An Int'l J.*, **5**(4).
- Tsai, C.S., Chiang, T.C. and Chen, B.J. (2005), "Component and shaking table tests for full-scale multiple friction pendulum system", *Earthq. Eng. Struct. Dyn.*, **35**, 1653-1675.
- Wang, J.F., Huang, M.C., Lin, C.C. and Lin, T.K. (2013), "Damage identification of isolators in Base-isolated torsionally coupled buildings", *Smart Struct. Syst., An Int'l Journal*, **11**(4).
- Zayas, V.A., Low, S.S. and Mahin, S.A. (1987), *The SFP Earthquake Resisting System: Experimental Report*, Report No. UCB/EERC-87/01, Earthquake Engineering Research Center, University of California Berkeley, Berkeley, CA, USA.
- Zayas, V.A., Low SS, Bozzo, L and Mahin S.A. (1989), *Feasibility and Performance Studies on Improving the Earthquake Resistance of New and Existing Buildings Using the Friction Pendulum System*, Report No. UCB/EERC-89/09, Earthquake Engineering Research Center, University of California Berkeley, Berkeley, CA, USA.